



HAL
open science

Characterization of swelling behavior and elastomer properties of acrylate polymers containing 2-ethylhexyl and isobornyl esters

Merah Dounya, Ulrich Maschke, Nouria Bouchikhi, Houcine Ziani Chérif,
Lamia Bedjaoui-Alachaher

► To cite this version:

Merah Dounya, Ulrich Maschke, Nouria Bouchikhi, Houcine Ziani Chérif, Lamia Bedjaoui-Alachaher. Characterization of swelling behavior and elastomer properties of acrylate polymers containing 2-ethylhexyl and isobornyl esters. *Polymer Bulletin*, 2022, *Polymer Bulletin*, 10.1007/s00289-022-04491-w . hal-03872003

HAL Id: hal-03872003

<https://hal.univ-lille.fr/hal-03872003>

Submitted on 19 Dec 2022

HAL is a multi-disciplinary open access archive for the deposit and dissemination of scientific research documents, whether they are published or not. The documents may come from teaching and research institutions in France or abroad, or from public or private research centers.

L'archive ouverte pluridisciplinaire **HAL**, est destinée au dépôt et à la diffusion de documents scientifiques de niveau recherche, publiés ou non, émanant des établissements d'enseignement et de recherche français ou étrangers, des laboratoires publics ou privés.

Characterization of swelling behaviour and elastomer properties of acrylate polymers containing 2-ethylhexyl and isobornyl esters

Merah Dounya^a, Ulrich Maschke^b, Nouria. Bouchikhi^{a,c}, Houcine. Ziani Chérif ^a, Lamia Bedjaoui-Alachaher^{a*}

^a*Laboratoire de Recherche sur les Macromolécules (LRM), Faculté des Sciences, Université Abou-bekr Belkaïd de Tlemcen (UABT), BP 119, 13000 Tlemcen, Algeria,*

^b*Unité Matériaux et Transformations – UMET (UMR CNRS N°8207), Bâtiment C6, Université de Lille - Sciences et Technologies, 59655 Villeneuve d'Ascq Cedex, France*

^c *Centre de Recherche Scientifique et Technique en Analyses Physico-chimiques (CRAPC). Zone Industrielle, BP 384, 42415 Bou-Ismaïl, Tipaza, Algeria*

*lamia.alachaher@univ-tlemcen.dz

ACCEPTED MANUSCRIPT

Characterization of swelling behaviour and elastomer properties of acrylate polymers containing 2-ethylhexyl and isobornyl esters

Abstract

In this work, a comparative study of the swelling behavior of poly (1, 7, 7-trimethyl-2-bicyclo [2.2.1] heptanyl) prop-2-enoate (poly (IBOA)) and its copolymer (poly (IBOA)-co-2-EHA), prepared by radical polymerization with the addition of a low concentration of crosslinking agent and photoinitiator, was performed. The obtained networks were characterized by FTIR to show the conversion of acrylic band before and after polymerization and by differential scanning calorimetry (DSC). The copolymer network has a single glass transition temperature (T_g) that decreases relative to the poly (IBOA). The swelling study of (poly (IBOA)-co-2-EHA) was carried out by gravimetric method, in a series of polar (methanol, ethanol, propan-1-ol, butan-1-ol, pentan-1-ol, hexan-1-ol and heptan-1-ol) and non-polar (toluene) isotropic solvents. Solubility, interaction and diffusion parameters that influence the swelling of copolymer in the solvents were calculated. The well-established order of swelling (toluene > heptan-1-ol > hexan-1-ol > pentan-1-ol > butan-1-ol > propan-1-ol > ethanol > methanol) in the copolymer was clearly observed and moreover the degree of swelling increased with the presence of EHA in the copolymer. A simple diffusion model was applied (Fick's model) to interpret the swelling data. It was found that the nature of solvent shifts the mechanism from diffusion-controlled in the case of alcohols to non Fickian one for toluene. For a long period, the experimental results were well correlated with the second order diffusion kinetics of Schott.

Graphical Abstract

Keywords: Swelling properties; organogels; properties and characterization.

1- Introduction

Understanding the swelling of small molecules in polymeric materials known as polymer gel, is important to advanced polymer technologies such as hydrogels [1-3], baby diapers [4], membranes [5-7], barrier materials [8], controlled drug release [9,10], shape memory polymers [11], adsorption of pollutant [12] and chemical sensors [13,14] as well as estimating the durability of polymers in contact with solvents.

Polymer gels or organogels represent a three-dimensional hydrophobic crosslinked polymer, which can retain a large amount of organic solvents without dissolving. The process of swelling of the solvent to a dry crosslinked polymer is conducted via the gradient of the chemical potential of the penetrant until thermodynamic equilibrium, in the polymer-solvent is reached. In general, rigidity/flexibility, hydrophilicity/hydrophobicity as well as the nature of polymer chains and solvent, sample preparation, degree of crosslinking and temperature have great influence on the swelling.

Gravimetric method has proven to be a reliable technique to determine the mass uptake of solvent by the crosslinked polymer [15]. It measures the total weight gain after exposure to liquid for a given time. Furthermore, from the obtained swelling curves, some important parameters can be deduced such as solubility parameter, polymer-solvent interaction, diffusion coefficient and kinetic parameters.

Lee et al [16] measured the swelling induced by a series of organic solvents in polydimethylsiloxane (PDMS) to examine the possibility of using this matrix in microfluidic devices, and found that solvent induced swelling decreases with the increase in the difference between the solubility parameter of the solvent and PDMS ($\delta - \delta_{PDMS}$).

G. Cocchi et al [17] determined the solubility and diffusion of several organic solvents in cross-linked PDMS membrane by a gravimetric method at 35°C. The effect of size, structure and solubility parameter of different molecules on sorption and transport properties in PDMS, were discussed. Indeed, in the case of alkanes, the weight-based solubility decreases with increasing solvent size due to entropic reasons while in the case of alcohols, the solubility of low molecular weight primary alcohols (ethanol, propan-1-ol, butan-1-ol) increases with the molecular size and with the length of the alkyl chain due to the decrease of unfavourable energetic interactions between the -OH groups of the alcohols and aliphatic groups of the polymer. From butan-1-ol to

hexan-1-ol, the solubility decreases with molecular size, indicating the entropic term prevails over the energetic one.

In the same research framework, S. Bedjaoui et al [18] performed swelling measurements of photochemically crosslinked poly (butylprop-2 enoate) (PABu) in linear primary alcohols. The increase of swelling of PABu from methanol to butan-1-ol reaching a maximum and subsequently the decrease from butan-1-ol to heptan-1-ol were also noted. In this case, the molecular simulation highlighted this trend in swelling behaviour.

The opposite effect was observed in polybenzimidazole at 25°C, as reported by Kelly P. Bye [19]. Polybenzimidazole was exposed for one week to both pure and mixed liquid (aliphatic and aromatic hydrocarbons, alcohols, water, and acetone). Interestingly the solubility of low molecular weight primary alcohols (methanol, ethanol, propan-1-ol) increases with decreasing alkyl chain length due to their favourable interaction (of enthalpic origin) via hydrogen bonding between polar –OH groups of alcohols and the –NH groups on the polymer backbone. On the other hand, the decrease in solubility observed for (butan-1-ol, hydrocarbons, PEG400) as a function of molar volume is attributed to entropic effects. Due to its hydrophilic structure, polybenzimidazole exhibits a completely opposite behaviour to hydrophobic PDMS (alcohols and hydrocarbons) and PABu (alcohols).

The main objective of this study is the preparation and characterization of novel polymeric materials for use in non-aqueous system. For this purpose, toluene and a series of alcohols were tested to follow the swelling of an amorphous copolymer with desired changes in thermal properties and swelling behaviour, compared to its homopolymers. To achieve this, a copolymer composed of 1, 7, 7-trimethyl-2-bicyclo [2.2.1] heptanyl prop-2-enoate (IBOA) and 2-ethylhexyl prop-2-enoate (2-EHA) designed by poly (IBOA-co-2-EHA) and its homopolymers poly (IBOA) and poly (2-EHA) were considered. Poly (IBOA) was chosen for its interesting physical properties: high glass transition temperature, shape recovery, tensile strength, high chemical resistance and excellent transparency. However for many applications, its swelling properties in organic solvents are limited especially at ambient temperature. Their modification could be therefore be obtained by elaboration of copolymer based on 2-EHA as co-monomer since its thermal and structural properties are different from those of IBOA.

In the present work, emphasis was placed on the study of swelling of toluene, methanol, ethanol, propan-1-ol, butan-1-ol, pentan-1-ol, hexan-1-ol and heptan-1-ol for the crosslinked copolymer poly (IBOA-co-2-EHA). Their elaboration can be initiated in many different ways [20, 21]. The free radical photo-polymerisation with UV light, involving crosslinking monomers was adopted. It offers several advantages, for instance, solvent free, fast curing time and easy application.

Solubility and diffusion values of toluene and alcohols in crosslinked poly (IBOA-co-2-EHA) were measured gravimetrically, at 25°C. The copolymer/solvent solubility and interaction parameters, and rate constant values were investigated.

2- Experimental part

a. Materials

The monofunctional monomers (1, 7, 7-trimethyl-2-bicyclo [2.2.1] heptanyl) prop-2-enoate (IBOA) and 2-ethylhexyl prop-2-enoate (2-EHA) were obtained from Sigma-Aldrich. The crosslinking agent 6-prop-2-enoyloxyhexyl prop-2-Enoate (HDDA) and the photo-initiator 2-hydroxy-2-methyl-1-phenyl-propan-1-one called Darocur 1173 were supplied by Cray Valley and Ciba Speciality Chemicals respectively. The selected solvents for this study are, toluene, methanol; ethanol, propan-1-ol, butan-1-ol, pentan-1-ol, hexan-1-ol and heptan-1-ol were purchased from Sigma Aldrich. Chemical structures of IBOA, 2-EHA and HDDA are presented in Fig 1.

Fig.1

b. Sample preparation

Disc-shaped crosslinked polymer samples of average dimension 3 x 0.15 cm were prepared using molds of appropriate dimensions. The diameter and thickness of all samples were measured using a micrometer to an accuracy of ± 0.001 mm and the weight of all samples was measured using an analytical balance to an accuracy of ± 0.0001 g. The samples were prepared by carrying out free radical polymerization of IBOA and 2-EHA to obtain the homopolymers and free radical co-polymerisation to obtain the copolymer using HDDA as crosslinking agent and Darocur as photo-initiator in both cases.

The pre-polymerization step consists of preparing solutions, composed of 1.1 mg of crosslinking agent and 4.1 mg of photo-initiator, dissolved in either 1.00 g of IBOA ($\rho = 0.986 \text{ g/cm}^3$) or 1.00 g of 2-EHA ($\rho = 0.885 \text{ g/cm}^3$) to prepare poly(IBOA) and poly(2-EHA) respectively. The poly (IBOA-co-2-EHA) copolymer was prepared by keeping the previous amounts of HDDA and Darocur constant and 0.60 g of IBOA and 0.40 g of 2-EHA were added. The different formulations expressed in mole percent are listed in Table 1.

The mixtures were mechanically stirred for 24 hours before pouring into teflon molds. The sample was exposed to UV light under nitrogen atmosphere for 30 minutes to achieve complete conversion of the monomers. As both IBOA and 2-EHA monomers are miscible at room temperature, no solvent was required to elaborate the networks. The irradiation process was carried out under nitrogen atmosphere ($P = 0.6 \text{ bar}$) using Philips TL08 UV lamps with a wavelength of $\lambda = 365 \text{ nm}$ and an intensity $I_0 = 1.5 \text{ mW/cm}^2$.

Table 1

c. Infrared measurements

Fourier Transform Infrared (FTIR) spectroscopy was performed in an attenuated total reflection (ATR) mode using an Agilent technologies model Cary 650 spectrophotometer. IR spectra were collected before and after photo-polymerization. At least 16 scans were performed for each measurement with wavelength resolution of 4 cm^{-1} . The acquired spectra were recorded over the spectral range of $500 - 4000 \text{ cm}^{-1}$.

d. DSC measurements

The calorimetric studies were carried out using a DSC 8500 calorimeter from Perkin Elmer Instruments, equipped with intra-cooler. The DSC equipment was calibrated using indium as standard. Heating and cooling rates of $10^\circ\text{C}/\text{min}$ were applied over the temperature range from -80°C to $+80^\circ\text{C}$ under nitrogen flow for three times. Measurements of the different thermal properties were always recorded during the second temperature cycle as the first cycle (heating-cooling) just eliminates the thermal history of the material. The glass transition temperatures (T_g) were determined from the inflection points of the thermograms and their values were given using a pyris manager software.

e. Swelling investigations

The solvent uptake during the swelling process was determined by gravimetric method [15]. A transparent sample with a diameter of 3.0 cm and a thickness of 1.5 mm was therefore immersed in different solvents at 25°C . At given time, the swollen gel was removed from the solvent with absorbent paper to remove the excess and was then weighed on the balance (accuracy $\pm 0.1 \text{ mg}$). The process was performed within a maximum of 30 seconds to minimize errors. The sample was returned to the solution and the procedure was repeated until swelling equilibrium was reached. The average value of three swelling experiments in each solvent for each sample was used. The swelling degree by weight (SD_t) was calculated according to equation 1.

$$SD_t = \frac{(w_t - w_0)}{w_0} \quad (1)$$

where w_0 represents the weight of the dried sample (initial state), and w_t stands for the weight of the swollen sample at a given immersing time t .

The equation 2 which is simple and useful, was used to determine the nature of the solvent diffusion in the gel (swollen copolymer) [22] :

$$\frac{SD_t}{SD_e} = k t^n \quad (2)$$

where: SD_t and SD_e are the swelling degree by weight at time t and equilibrium, respectively. The constants « n » and « k » are characteristic of the solvent-copolymer system. The exponent « n » indicates the type of the diffusion of the solvent inside the copolymer network and « k » is a function of polymer type and nature of the solvent molecule, related to both the diffusion parameters and the copolymer-solvent interactions. This equation is applied to the initial swelling data when values SD_t / SD_e are less than 0.6.

The swelling rate of the gels when the SD_t / SD_e values for the entire swelling time can be described with Schott's second-order swelling kinetics [23]. The equation is as follows:

$$\frac{dSD_t}{dt} = k'(SD_e - SD_t)^2 \quad (3)$$

k' represents the swelling rate coefficient. The integration of equation (3) between the limits $SD_t = 0$ when $t = 0$ and SD_t for t , leads to:

$$\frac{1}{(SD_e - SD_t)} - \frac{1}{SD_e} = k't \quad (4)$$

Further linearization gives:

$$\frac{t}{SD_t} = \frac{1}{SD_e} t + \frac{1}{k'SD_e^2} \quad (5)$$

Here, k' is the swelling rate constant; and $k'SD_e^2$ is the initial swelling rate (r_0).

3- Results and discussion

The elaboration of cross-linked, poly (2-EHA), poly (IBOA) and poly (IBOA-co-2-EHA) was rationally designed by using their corresponding acrylic monomers, 2-EHA, IBOA and as crosslinker HDDA in the presence of the photoinitiator Darocur.

A low crosslinking density was intentionally targeted to allow a large solvent diffusion into the matrix. Indeed, it was assumed that the swelling process would be driven by hydrophobic interactions between the solvent and the polymer network. This assumption was supported by previous experimental results from our group [18]. In an attempt to visualize the polymer network and its subsequent interaction with the solvent, an energy-minimized computer-generated 3D representation model of 40 poly (2-EHA) and poly (IBOA) units is illustrated in Figure 2. Salient features supporting our assumption are retrieved from Figure 2. The polar ester groups of the main polymer backbone are deeply enfolded within the network making access or any dipolar interaction of polar molecules hardly possible. Hydrophobic pendant groups thus surround the polar groups. In addition, all the pendant groups present in the three polymer networks are hydrophobic in nature and extend towards the external surface of the network. This is particularly important to consider, as our materials were prepared by a bulk polymerization mode and hence one can easily imagine that it tends to obtain a polymer network where hydrophobic groups are oriented towards the external surface in order to minimize the interfacial surface energy.

Fig. 2

Regardless of the free volume available in all polymer networks and the conformational distortions of the pendant groups, it appears from Figure 2 that swelling will occur preferentially in non-polar solvents. Among the solvents under investigation in this study and in their liquid state, toluene can be expected to be the best penetrating solvent owing to hydrophobic interactions with hexyl or isobornyl groups. Alcohols bearing a long hydrocarbon chain ($> C_4$) are considered hydrophobic since they barely dissolve in water even though they have a polar hydroxyl group. The size, composition and physico-chemical properties of this architecture will be crucial in the swelling process in terms of interaction, rate and diffusion in the free volume. Some thermodynamic and kinetic aspects of swelling will be investigated in the following.

a. FTIR analysis

The FTIR spectra ($750\text{-}3000\text{ cm}^{-1}$) of the monomers 2-EHA, IBOA and the mixture IBOA/2-EHA and their corresponding polymers are shown in Figure 3. Infrared spectra of monomers contain expected peaks, the band observed around 1720 cm^{-1} is assigned to the stretching vibration of conjugated ester -C=O ; the bands observed around 1050 and 1200 cm^{-1} are attributed to the $\text{-CH}_2\text{-O}$ and acyl group (C-O) functions respectively [24]. Medium bands between 1375 and 1400 cm^{-1} correspond to asymmetric and symmetric bending vibration of methyl group and a characteristic band corresponding to the acrylic group (C=C) is observed at 810 cm^{-1} and 1635 cm^{-1} .

Photopolymerization of poly (IBOA), poly (2-EHA) and poly (IBOA-co-2-EHA) occurred in the presence of HDDA and Darocur upon UV exposure. The signal located at 810 cm^{-1} enabled to monitor

polymerization/crosslinking processes and to evaluate monomer conversion. Indeed this signal disappears when C=C bonds have been consumed. To ensure complete conversion, the mixtures were exposed for 30 min to UV lights. Inserts a, b and c in Figure 3, show the zoomed area of IR spectra between the wavelength of 750 – 830 cm^{-1} for 2-EHA, IBOA/2-EHA mixture and IBOA, respectively. The estimated conversion were made by measuring the peak heights of the absorption band at 810 cm^{-1} before ($t=0$) and after UV exposure ($t=30$ min). The calculated conversions were approximately 97% for poly (2-EHA), 95% for poly (IBOA-co-2-EHA) and 93% for poly (IBOA) indicating an almost complete consumption of C=C double bonds.

Fig. 3

b. Thermal analysis

Representative DSC heat flow curves normalized by sample mass of poly (IBOA), poly (2-EHA) and poly (IBOA-co-2-EHA) are collected in Figure 4. Pure poly (IBOA) exhibits single glass transition temperature (T_g) at about 48°C whereas pure poly (2-EHA) is marked essentially by its very low glass transition temperature at -66° C (see table 2) [25]. The difference in glass transition temperatures between poly (IBOA) and poly (2-EHA) is due to the chemical structures of the two homopolymers, IBOA has rigid bicyclic structure and 2-EHA having flexible chain.

Table 2

A single glass transition temperature between those of the corresponding homopolymers, is also observed in the case of poly (IBOA-co-2-EHA) ($T_g = 4^\circ\text{C}$) indicating the formation of a random copolymer. These results were previously reported by Zeggai et al [26] for poly (IBOA-co-IsoBA), where they were able to lower the glass transition temperature of poly IBOA from 46.3°C to 45.2°C by copolymerization with isobutyl acrylate (IsoBA), with a composition of (IBOA/IsoBA =4/1 weight ratio). Shojaei et al [27] synthesized copolymers of acrylic acid AA and 2-EHA with different compositions, and the glass temperatures of the copolymers were between those of poly (AA) and poly (2-EHA), and decreased as the amount of 2-EHA monomer increased.

Fig. 4

c. Swelling behavior

The swelling properties of poly (IBOA-co-2-EHA) were determined by immersing it in several solvents. From the photos in Figure 5, it can be seen that the swelling behaviour in toluene is fast but not uniform, so the swelling process can be divided into three parts: From $t = 0$ min to 5 min, the absorption takes place only at the edge, as the elastomer is rigid at the beginning of swelling and the contact with solvent progressively reduces its rigidity. From $t = 10$ min to 15 min, a deformation is observed in the middle of the sample. It could be explained by the presence of a geometrical constraint due to the presence of the bicyclic structure of IBOA in contact with the ring constituting toluene. In this case the shape of the sample changes and the swelling is unidirectional. This inhomogeneity during swelling was observed by Tanaka [28,29] and also confirmed by J. Dervaux et al [30]. They found that when a gel sample (polyacrylamide) is immersed in a solvent (water), sharp folds quickly appear over the entire gel surface. As the solvent diffuses, the characteristic spacing between these folds increases with time until they finally disappear, ie when the gel surface becomes homogeneous. This corresponds to the last step shown at $t = 30$ min where the absorption is uniform in all directions. At equilibrium, the gel becomes flat, flexible, and sensitive, by simple contact, it can be cut into small pieces after 24 hours.

Fig. 5

In the case of the alcoholic solvents, the diffusion of solvents molecules is uniform which is probably due to the duration of the swelling process (8 days), which allows the elastomeric chain to stretch slowly and therefore the solvent can diffuse in all directions without causing geometric stress or shape deformation. Photos of the first times of poly (IBOA-co-2-EHA) in alcohols are not shown as no change was observed.

The swelling degree (SD_t) as function of time is shown in Figure 6. The well-established order of swelling (toluene > heptan-1-ol > hexan-1-ol > pentan-1-ol > butan-1-ol > propan-1-ol > ethanol > methanol) can be clearly observed. The time needed to achieve the swelling equilibrium varies depending on the system: polymer/polar solvent (case of alcoholic solvents) and polymer/non-polar solvent (case of toluene). For example, toluene causes significant swelling, and the plateau is reached after 2 days while for alcohols it is reached after 8 days.

Compared to heptan-1-ol, hexan-1-ol and butan-1-ol, the amount of solvent inside the gel in the case of toluene is 2.2 times higher. Using methanol as solvent, almost no swelling could be observed. The low uptake of

methanol could be attributed to its high polarity, which may limit its diffusion into non-polar copolymer. Conversely, non polar toluene has an affinity for the copolymer.

Fig. 6

In order to examine the effect of 2-EHA content in the copolymer on the swelling properties, only toluene and heptan-1-ol were tested. The swelling behavior of poly (IBOA-co- 2-EHA) and its homopolymers was presented in Figure 7, which shows that the swelling degree of the copolymer is between that of poly (IBOA) and poly (2-EHA) for toluene and heptan-1-ol. In both solvents, poly (IBOA) is the least swollen.

These results are explained by the fact that the addition of 2-EHA increases the viscosity of the copolymer thus producing a flexible network of macromolecular chains. This obviously leads to a rapid diffusion of toluene and heptan-1-ol into the copolymer ($T_g = 4^\circ\text{C}$) and consequently the swelling rate increases compared to poly (IBOA). It was also noticed that the uptake masses of toluene and heptan-1-ol are 2 times higher in poly (IBOA-co-2-EHA) than in poly (IBOA). Moreover, the high rigidity of the poly (IBOA) network ($T_g = 48^\circ\text{C}$) also restricts the movement or relaxation of macromolecular chains in the matrix thus allowing slower diffusion of the solvent into the gels.

Fig. 7

d- Swelling thermodynamics

Solubility parameter

Swelling behavior can also be predicted using the solubility parameters [31]. It has been found that the squared difference between polymer and solvent solubility parameters plays a key role in predicting the degree of swelling in pure solvents. Swelling is maximal when $(\delta_s - \delta_p)^2$ is equal to 0. It is therefore well known that there are several common features between the swelling behavior of a lightly crosslinked polymer in solvent and the dissolving of the linear polymer in solvent. A solvent that can dissolve a linear polymer could also swell the polymer network. Therefore, the swelling of copolymer networks would conform to the dissolution rules of linear copolymers or the Hildebrand equation [32]:

$$\Delta H_M / (V\varphi_s\varphi_{cop}) = (\delta_s - \delta_{cop})^2 \quad (6)$$

where ΔH_M is the enthalpy change when mixing polymer and solvent, V is the total volume of the solution, φ_s and φ_{cop} are the volume fractions for solvent and copolymer, and δ_s and δ_{cop} are the solubility parameters for solvent and copolymer. Using equation (6), the affinity between the solvent and the copolymer can be predicted if the solvent and polymer solubility parameters are close to each other.

The Hildebrand solubility parameters δ_s , δ_1 and δ_2 are those of the solvent, poly (IBOA) and poly (2-EHA) respectively, can be estimated according to Fedors' method [33] using equation (7).

$$\delta = \frac{\sum_i \Delta e_i}{\sum_i \Delta v_i} \quad (7)$$

where, Δe_i and Δv_i are the additive atomic and group contribution for the energy of vaporization and molar volume, respectively. Hildebrand solubility parameters are estimated: $\delta_1 = 16.1 \text{ (J/cm}^3\text{)}^{1/2}$ for poly (IBOA) is and $\delta_2 = 19.0 \text{ (J/cm}^3\text{)}^{1/2}$ for poly (2-EHA). The solubility parameter of the poly (IBOA-co-2-EHA) could be calculated from the following equation [34]:

$$\delta_{cop} = \varphi_1\delta_1 + \varphi_2\delta_2 \quad (8)$$

where, ϕ_1 (0.57) and ϕ_2 (0.43) are the volume fractions of IBOA and 2-EHA in the copolymer. The theoretical value is $\delta_{\text{cop}} = 17.3 \text{ (J/cm}^3\text{)}^{1/2}$. The calculated solubility parameters δ_s of all solvents according to Fedor's method are reported in table 3. The higher solubility parameters of solvents led to lower swelling values. Thus the greatest swelling is obtained in the presence of toluene ($\delta_s = 18.3 \text{ (J/cm}^3\text{)}^{1/2}$) while the lowest one is obtained in the presence of methanol $\delta_s = 28.2 \text{ (J/cm}^3\text{)}^{1/2}$). Furthermore the estimated solubility parameter of copolymer $\delta_{\text{cop}} = 17.3 \text{ (J/cm}^3\text{)}^{1/2}$ is close to that of toluene indicating its high swelling in this solvent.

For the solvents used in this study, dispersion, polar and hydrogen bond parameters were also considered according to the Hansen method [35] (see table 3).

A key observation from table 3 is that the seven alcohols have similar dispersion values (though that of methanol is slightly lower), but that polar and hydrogen bonding parameters decrease with increasing chain length. The latter has the effect of reducing the strength of polarity and hydrogen bonding. Pentan-1-ol and hexan-1-ol differ from the linear alcohols in having a slightly higher polar solubility parameter. In the series of alcohols, methanol has higher value of δ_h and δ_p and is therefore the most polar solvent. Conversely, toluene is non polar due to its low polarity and hydrogen bonding values.

Table 3

Another observation deduced from Figure 6 is that the swelling of poly (IBOA-co-2-EHA) increases with the chain length of alcohols. This effect is attributed to the decrease in polarity and hydrogen bonding. Toluene which has the lowest polarity and hydrogen bonding, gave the highest swelling of the copolymer. These swelling results are consistent with the predicted solubility.

Copolymer-solvent interaction parameter

Swelling equilibrium studies were also developed to evaluate the interaction parameter between the copolymer and solvent. For this, the classical Flory-Huggins theory was considered as it has been proven to be a valid theory for many copolymer-solvent systems, especially for elastomeric materials swollen by good solvents [36]. The starting point is equation (9), which gives solvent activity in a copolymer at equilibrium in the case of a binary (copolymer/solvent) system.

$$\ln a_s = \ln \phi_s + \left(1 - \frac{V_s}{V_{\text{cop}}}\right) \phi_{\text{cop}} + \chi_{\text{scop}} \phi_{\text{cop}}^2 \quad (9)$$

where, a_s : denoted the solvent activity, ϕ_s and ϕ_{cop} are volume fractions of solvent and copolymer, V_s and V_{cop} are molar volumes of solvent and copolymer and χ_{scop} the Flory-Huggins interaction parameter. The volume fraction must satisfy the balance $\phi_s + \phi_{\text{cop}} = 1$. The copolymer volume fractions were calculated from the equilibrium swelling of the copolymer in different solvents. Assuming that $V_{\text{cop}} \gg V_s$ and $a_s = 1$ based on swelling a copolymer in pure solvent [37], the copolymer-solvent interaction parameter χ_{scop} can be obtained using the equation (10).

$$\chi_{\text{scop}} = -\frac{\ln \phi_s + \phi_{\text{cop}}}{\phi_{\text{cop}}^2} \quad (10)$$

The χ_{scop} parameter can be used to determine qualitatively whether or not the liquid is a non-solvent ($\chi_{\text{scop}} > 1$), a solvent or plasticizer ($0.5 < \chi_{\text{scop}} < 1$) or a good solvent ($\chi_{\text{scop}} \leq 0.5$) [38].

The Flory Huggins interaction parameter χ can also be calculated using regular solution theory, shown in equation (11) [39,40]:

$$\chi = 0.34 + \frac{V_s}{RT} (\delta_{\text{cop}} - \delta_s)^2 \quad (11)$$

Table 4

The solvent volume fraction ϕ_s and copolymer-solvent interaction χ_{scop} for different solvents, at equilibrium are presented in table 4. The trend shows that the highest ϕ_s is obtained with the most swollen copolymer because it contains a large amount of solvent. In this case, the solvent volume fraction of toluene is 0.911 and that of methanol is 0.114. Considering the alcohols series, the solvent volume fraction increases from methanol to butan-1-ol and changes slightly from pentan-1-ol to heptan-1-ol.

On the other hand, the lowest interaction parameter is 0.53 for toluene and the highest interaction parameter is 1.64 for methanol. In general, the interaction parameter increases with increasing solubility parameters of pure solvents. These results are in agreement with the swelling results for these solvents, and indicate that the higher the swelling degree, the lower the interaction parameter. The results also show that the value of interaction parameters could be used to identify the compatibility between polymer and solvent as well as δ_p and δ_h .

In addition, the Flory Huggins interaction parameters χ calculated according to regular solution theory, are high compared to those determined from the swelling study (χ_{scop}). It can be deduced that the copolymer-solvent interaction becomes increasingly favourable when the poly (IBOA-co-2-EHA) is swollen by alcohols. Bae et al [41] have experimentally shown that this interaction varies with polymer-solvent concentration. However, for toluene, a slight increase ($\chi > \chi_{scop}$) is noted; this could be due to the presence of phenyl in contact with the bicyclic structure of IBOA.

Figure 8 displays the swelling degree of the copolymer immersed in different solvents and the interaction parameter as function of solvent solubility parameter, at T=25°C. The results show that solvents with higher solubility parameters produce lower swelling values, which means that as the solvent solubility parameters increase, the interactions with the copolymer become less favourable.

Fig. 8

On the other hand the interaction copolymer-solvent parameter χ_{scop} decreases when solvent solubility parameters decrease. The closer the value of χ_{scop} is near to 0.5, the better the solvent quality. Hence, toluene interaction with copolymer is the highest, followed by heptan-1-ol, hexan-1-ol, pentan-1-ol, butan-1-ol, propan-1-ol, ethanol and methanol. Unfavourable interactions between methanol molecule and copolymer can have significant energetic contributions to the mixing process, resulting in low concentration within the copolymer. As suggested previously, this large difference may be related to the fact that methanol is polar.

To better understand the effect of the nature of the solvent on the swelling behavior, Figure 9 shows photos of the swollen copolymer only in methanol ($\chi_{scop} > 1$) and heptan-1-ol ($\chi_{scop} < 1$) after one week. At equilibrium, opacity was clearly observed when the material was soaked in methanol while in heptan-1-ol, it was optically transparent. These observations suggest that methanol molecules accentuate solvent clustering in copolymer.

Fig. 9

Indeed alcohols have ability to form multiple hydrogen bond through their hydroxyl groups and therefore form clusters in contact with hydrophobic polymers. Clustering occurs when solvent molecules have strong affinity to each other compared to the solvent-polymer affinity. The solvent-solvent affinity decreases with the increase of carbon chain in alcohols showing a greater swelling with poly (IBOA-co-2-EHA). Favre et al [42] highlighted, using FTIR-ATR, the formation of methanol clusters in contact with hydrophobic polymers like PDMS.

From the above analysis, it can be concluded that the highest swelling degree was obtained when the solvent solubility parameter is close to that of the poly (IBOA-co-2EHA) ie the difference in the interaction parameter between the solvent and the polymer is lower. Consequently, the value of the copolymer solubility parameter can be predicted by experiment. Furthermore, methanol and ethanol are more likely to form solvent clusters in the copolymer than the others alcohols.

e- Swelling kinetics

The rate of solvent uptake by a polymer can be limited by two different processes: the diffusion rate of the solvent in the polymer and the relaxation of the polymer chains. These relaxations are a direct result of the solvent-induced swelling of the material. These two processes can be superimposed and therefore lead to multiple theoretical swelling curves [43]. Since the diffusion of organic matter cannot control the whole swelling process, the interpretation of mechanism for the first swelling time was then provided by the Fick's model whereas the

overall kinetics of a hydrogel, involving long swelling periods, may be described with Schott's second-order swelling kinetics.

Initial swelling

Based on equation (2), the n and k values were calculated from the slopes and intercepts of the plot $\ln SD_t/SD_e$ versus $\ln t$ for the results shown in Figure 6, for swelling of poly (IBOA-co-2-EHA) in different solvents at 25°C, and reported in Table 5. It was observed that the nature of solvent shifts the mechanism from diffusion control to non Fickian mechanism. Indeed, values of n ranging from 0.25 to 0.46 were noted for alcohols while the value of n was higher than 0.5 for toluene. Indeed, the Fickian diffusion indicates that the diffusion rate of alcohols in the gel is lower than the relaxation rate of the polymer chain, so n close to 0.45 signifies a Fickian process [44]. However, methanol and ethanol have lower n (<0.45) but these cases are still considered as Fickian diffusion, so it is referred to as less Fickian diffusion. As mentioned in previous studies [45] for dihydroxypropyl methacrylate hydrogel, n can reach a value as low as 0.32 and for an interpenetrating polymer network comprising hydrophilic and hydrophobic chains, n can even reach a lower value of 0.18 [46]. On the other hand, non Fickian diffusion of toluene occurs when the diffusion and relaxation rates are comparable and gel swelling is controlled by both solvent diffusion within the copolymer matrix and relaxation of copolymer chains. In the alcohol series, the value of k tends to decrease from methanol to butan-1-ol but is almost constant up to heptan-1-ol. Furthermore the coefficients of determination (R^2) shift away from linearity indicating that the diffusion was not the only rate-limiting step, but that other processes control the swelling rate [47]. The solvent diffusion coefficient in gels (D) can also be discussed; it can be determined by many methods, one of which is the short-time approximation method, which is the most commonly applied. This method is only used for the first 60% of swelling, during which the polymer thickness basically remains constant. D can be calculated using equation (11) [48]:

$$\frac{SD_t}{SD_e} = \frac{4}{\sqrt{\pi}} \sqrt{\frac{Dt}{d^2}} \quad (11)$$

where d is the thickness of the gel. Based on the linear relationship between SD_t and $t^{1/2}$, the values of D were calculated from the slopes θ of these lines. Thus, D can be calculated from (12) by rearranging equation (11).

$$D = \pi \left(\frac{d\theta}{4SD_e} \right)^2 \quad (12)$$

The D values are also listed in Table 5. As expected, low molecular weight molecules show significantly higher diffusion coefficients than high molecular weight alcohols. The diffusion parameter decreases from methanol to pentan-1-ol and remains constant up to heptan-1-ol.

The swelling behavior of poly (IBOA-co-2-EHA) in alcohols as presented in Figure 6 could be easily explained by the fact that from methanol to heptan-1-ol, the increase in polymer-alcohol chemical affinity, which favors diffusion, is sufficient to compensate for the corresponding increase in stereochemical hindrance, which unfavors diffusion, involved in the diffusion of the longer solvent chains. This supports similar experiments observed on the diffusion of linear alcohols in amorphous polystyrene [49].

However the non-polar solvent (toluene) has a very high D value compared to alcohols. This peculiar diffusion behavior is certainly related to the high swelling of poly (IBOA-co-2-EHA) in toluene.

Table 5

Extensive swelling

Two kinetic models, commonly used in the literature, were applied to kinetic experimental data in order to study the behavior of solid liquid phases. These models are the Berens–Hopfenberg first order and the Schott second order equations. The validity of each model can be checked from the linear plot. To find the order of kinetics, the Berens–Hopfenberg equation was first tested but straight lines could not be obtained (results not shown). For the Berens–Hopfenberg plots, the coefficients of determination varied from 0.952 for toluene to 0.759 for heptan-1-ol. The inapplicability of the Berens–Hopfenberg equation to describe the swelling kinetics of organic solvents

using a methacrylic copolymer was also observed in a previous work [50]. It was reported that, after a short period, the experimental data deviated considerably from linearity (the model did not fit the data well for the whole contact time range). The pseudo-second order model involving long period, proposed by Schott was very efficient in correlating the experimental data for swelling kinetics as shown in Figure 10. The rate parameters k' and the degree of equilibrium swelling SD_e can be directly obtained from the intercept and slope of the plot of t/SD_e versus t . Very good straight lines were obtained for the different solvents, indicating that this kinetic model suggests that the swelling rate of the polymer matrix is controlled by solvent diffusion and polymer chain relaxation. Furthermore coefficient of determination (R^2) in Table 6 are higher than 0.98. The SD_e calculated from the slope of the straight lines are also in good agreement with the experimental swelling degree as displayed in Table 6. It can be noticed that the relative error between theoretical and experimental value is lower for methanol (1.8%), ethanol (0.7%), propan-1-ol (3.4%) and toluene (2.8%) whereas it is higher for butan-1-ol (6%), pentan-1-ol (9%), hexan-1-ol (9.9%) and heptan-1-ol (10%). This may be due to the fact that the copolymer need to be soaked in solvents for more than a week to reach equilibrium while for methanol, ethanol, propan-1-ol and toluene, one day was sufficient. In the alcohol series, the value of k' tends to decrease drastically from methanol to butan-1-ol but is almost constant up to heptan-1-ol. It can be concluded that methanol has fast diffusion at the early stage in the copolymer. The value of k' is higher for toluene than butan-1-ol suggesting a larger affinity of toluene with the copolymer compared to butan-1-ol.

Table 6

Fig. 10

4- Conclusions

This paper focuses on the development of a novel copolymer system by free radical polymerization of IBOA and 2-EHA. Structural analysis, thermal properties and swelling behavior in a series of organic solvents were studied. The degree of conversion of poly (IBOA-co-2-EHA) was improved compared to its homopolymer poly (IBOA), and the appearance of a single T_g confirms the homogeneous character of the resulting random copolymer. This glass transition temperature was considerably lower than that of poly (IBOA).

Swelling studies of poly (IBOA-co-2-EHA) in toluene show a typical behavior with a high degree of swelling compared to alcoholic solvents.

A clear correlation between the swelling degree and the solubility parameter was found: the higher the differences between the solvent and copolymer solubility parameters, the lower the degree of swelling of poly (IBOA-co-2-EHA). Indeed, methanol showed the lowest swelling within the copolymer as well as the highest Flory–Huggins parameter, meaning that the copolymer is selective towards this component. Furthermore, the diffusion process of alcohols follows the Fickian diffusion law while toluene shows an anomalous diffusion.

The first-order kinetic model was not suitable to describe the swelling process, but the second-order kinetic equation can describe it very well. The swelling rate of the polymer matrix is controlled by solvent diffusion and relaxation of the polymer chains.

DECLARATION OF COMPETING INTEREST

The authors declare that they have no known competing financial interests or personal relationships that could have appeared to influence the work reported in this paper.

ACKNOWLEDGEMENTS

This report has been accomplished in the framework of an international research program. The authors gratefully acknowledge the support of the Algerian Ministry of Higher Education and Scientific Research (MESRS), the General Directorate of Scientific Research and Technological Development (DGRSDT) of Algeria, the University of Tlemcen in Algeria, the CNRS, and the University of Lille – Sciences and Technologies/France.1.

REFERENCES

- [1] Wei, C et al (2018) The kinetics of the polyacrylic superabsorbent polymers swelling in microalgae suspension to concentrate cells density. *Bioresource technol* 249: p. 713-719. <https://doi.org/10.1016/j.biortech.2017.10.066>

- [2] Zhang, S.-X et al (2017) Determination of the swelling behavior of superabsorbent polymers by a tracer-assisted on-line spectroscopic measurement. *Polym Testing* 62: p. 110-114. <https://doi.org/10.1016/j.polymertesting.2017.06.020>
- [3] Basta, A.H., V.F. Lotfy, and C. Eldewany (2021) Comparison of Copper-crosslinked Carboxymethyl Cellulose Versus Biopolymer-based Hydrogels for Controlled Release of Fertilizer. *Polymer-Plastics Technology and Materials* 60 (17): p. 1884-1897. <https://doi.org/10.1080/25740881.2021.1934017>
- [4] Ni, C. and X.-X, Zhu (2004) Synthesis and swelling behavior of thermosensitive hydrogels based on N-substituted acrylamides and sodium acrylate. *Euro J Polym* 40(6): p. 1075-1080. <https://doi.org/10.1016/j.eurpolymj.2003.12.017>
- [5] Freeman, B., Y. Yampolskii, and I. Pinnau (2006) *Materials science of membranes for gas and vapor separation*. John Wiley & Sons.
- [6] Vieth, W.R. (1991) *Diffusion in and through polymers: principles and applications*. American Scientist;(United States), 81(1).
- [7] Neogi, P. (1996) *Diffusion in polymers*, Marcel Dekkers. Inc, New York.
- [8] Zemez, M., L. Vinches, and S. Hallé (2021) Molecular sorption and diffusion of organic solvents through maleated rubber/layered silicate nanocomposites. *Journal of Elastomers & Plastics*, p. 00952443211006162Yvhbn. <https://doi.org/10.1177/00952443211006162>
- [9] Yin, Y., Y. Yang, and H. Xu (2002) Swelling behavior of hydrogels for colon-site drug delivery. *J Appli Polym Sci* 83 (13): p. 2835-2842. <https://doi.org/10.1002/app.10259>
- [10] Li, Yet al (2022) Preparation of pH-responsive cellulose nanofibril/sodium alginate based hydrogels for drug release. *Journal of applied polymer science* 139(7): p. 51647. <https://doi.org/10.1002/app.51647>
- [11] Liu, M et al (2019) Ionic liquids as an effective additive for improving the solubility and rheological properties of hydrophobic associating polymers. *J Molecul Liquids* 296: p. 111833. <https://doi.org/10.1016/j.molliq.2019.111833>
- [12] Karadağ, E et al (2021) Swelling equilibria of novel propenamide/2-acrylamido-2-methyl-1-propanesulfonic acid/guar gum/clinoptilolite biohybrid hydrogels and application as a sorbent for BVI removal. *Polym Bull* 78(7): p. 3625-3649. <https://doi.org/10.1007/s00289-020-03285-2>
- [13] Igarashi, S et al (2006) Swelling signals of polymer films measured by a combination of micromechanical cantilever sensor and surface plasmon resonance spectroscopy. *Sensors and Actuators B: Chemical* 117(1): p. 43-49. <https://doi.org/10.1016/j.snb.2005.11.001>
- [14] Tillman, E.S. and N.S. Lewis (2003) Mechanism of enhanced sensitivity of linear poly (ethylenimine)-carbon black composite detectors to carboxylic acid vapors. *Sensors and Actuators B: Chemical* 96(1-2): p. 329-342. [https://doi.org/10.1016/S0925-4005\(03\)00567-7](https://doi.org/10.1016/S0925-4005(03)00567-7)
- [15] Liu, J., X. Zheng, and K. Tang (2013) Study on the gravimetric measurement of the swelling behaviors of polymer films. *Rev. Adv. Mater. Sci* 33(5): p. 452-458.
- [16] Lee, J.N., C. Park, and G.M. Whitesides (2003) Solvent compatibility of poly (dimethylsiloxane)-based microfluidic devices. *Analytical chemistry* 75(23): p. 6544-6554. <https://doi.org/10.1021/ac0346712>
- [17] Cocchi, G., M.G. De Angelis, and F. Doghieri (2015) Solubility and diffusivity of liquids for food and pharmaceutical applications in crosslinked polydimethylsiloxane (PDMS) films: I. Experimental data on pure organic components and vegetable oil. *Journal of Membrane Science* 492: p. 600-611. <https://doi.org/10.1016/j.memsci.2015.04.063>

- [18] Bedjaoui, S et al (2020) Unusual swelling of acrylate based crosslinked polymer networks in linear primary alcohols: Experimental and modeling aspects. *J Molecul Liquids* 320: p. 114459. <https://doi.org/10.1016/j.molliq.2020.114459>
- [19] Bye, K.P et al (2019) Pure and mixed fluid sorption and transport in Celazole® polybenzimidazole: Effect of plasticization. *J Membr Sci* 580: p. 235-247. <https://doi.org/10.1016/j.memsci.2019.03.031>
- [20] Odian, G (1991) *Principles of Polymerization*, 3rd; John Wiley&Sons. Inc, New York.
- [21] Bouchikhi, N et al (2019) Photo-curing kinetics of hydroxyethyl acrylate (HEA): synergetic effect of dye/amine photoinitiator systems. *Int J Indu Chem*, p. 1-9. <https://doi.org/10.1007/s40090-019-00197-7>
- [22] Peppas, N.A. and N.M. Franson (1983) The swelling interface number as a criterion for prediction of diffusional solute release mechanisms in swellable polymers. *J Polym Sci: Polym Phys Edition* 21(6): p. 983-997. <https://doi.org/10.1002/pol.1983.180210614>
- [23] Rudzinski, W. and W. Plazinski (2009) On the applicability of the pseudo-second order equation to represent the kinetics of adsorption at solid/solution interfaces: a theoretical analysis based on the statistical rate theory. *Adsorption* 15(2): p. 181-192. <https://doi.org/10.1007/s10450-009-9167-8>
- [24] Chatzi, E.G et al (1997) Infrared spectra and compositional analysis of styrene/2-ethylhexyl acrylate copolymers. *Macromol Chem and Phys* 198(8): p. 2409-2420. <https://doi.org/10.1002/macp.1997.021980805>
- [25] Boudraa, K., T. Bouchaour, and U. Maschke (2020) Thermal analysis of interpenetrating polymer networks through molecular dynamics simulations: a comparison with experiments. *Journal of Thermal Analysis and Calorimetry* 140(4): p. 1845-1857. <https://doi.org/10.1007/s10973-019-08898-y>
- [26] Zeggai, N et al (2018) Analysis of dynamic mechanical properties of photochemically crosslinked poly (isobornylacrylate-co-isobutylacrylate) applying WLF and Havriliak-Negami models. *Polym Testing* 72: p. 432-438. <https://doi.org/10.1016/j.polymertesting.2018.10.038>
- [27] Shojaei, A.H., J. Paulson, and S. Honary (2000) Evaluation of poly (acrylic acid-co-ethylhexyl acrylate) films for mucoadhesive transbuccal drug delivery: factors affecting the force of mucoadhesion. *J Contro Relea* 67(2-3): p. 223-232. [https://doi.org/10.1016/S0168-3659\(00\)00216-9](https://doi.org/10.1016/S0168-3659(00)00216-9)
- [28] Tanaka, T (1986) Kinetics of phase transition in polymer gels. *Physica A: Statistical Mechanics and its Applications* 140(1-2): p. 261-268. [https://doi.org/10.1016/0378-4371\(86\)90230-X](https://doi.org/10.1016/0378-4371(86)90230-X)
- [29] Tanaka, T et al (1987) Mechanical instability of gels at the phase transition. *Nature* 325(6107): p. 796-798. <https://doi.org/10.1038/325796a0>
- [30] Dervaux, J. and M.B. Amar (2012) Mechanical instabilities of gels. *Annu. Rev. Condens. Matter Phys* 3(1): p. 311-332. <https://doi.org/10.1146/annurev-conmatphys-062910-140436>
- [31] Burke, J (1984) *Solubility parameters: theory and application*.
- [32] Barton, A (1991) Expanded cohesion parameters. Chapter 5. *Handbook of solubility parameters and other cohesion parameters*.
- [33] Fedors, R.F (1974) A method for estimating both the solubility parameters and molar volumes of liquids. *Polym Eng & Sci* 14(2): p. 147-154. <https://doi.org/10.1002/pen.760140211>
- [34] Şen, M. and O. Güven (1998) Determination of solubility parameter of poly (N-vinyl 2-pyrrolidon/ethylene glycol dimethacrylate) gels by swelling measurements. *J Polym Sci Part B: Polym Phys* 36(2): p. 213-219. [https://doi.org/10.1002/\(SICI\)1099-0488\(19980130\)36:2%3C213::AID-POLB2%3E3.0.CO;2-S](https://doi.org/10.1002/(SICI)1099-0488(19980130)36:2%3C213::AID-POLB2%3E3.0.CO;2-S)
- [35] Hansen, C.M (2007) *Hansen solubility parameters: a user's handbook*: CRC press. <https://doi.org/10.1201/9781420006834>

- [36] TrongáNguyen, Q (1993) Sorption of organic solvents into dense silicone membranes. Part 1.—Validity and limitations of Flory–Huggins and related theories. *J Chem Society, Faraday Transactions* 89(24): p. 4339-4346. <https://doi.org/10.1039/FT9938904339>
- [37] Ferrell, W.H., D.I. Kushner, and M.A. Hickner (2017) Investigation of polymer–solvent interactions in poly (styrene sulfonate) thin films. *J Polym Sci Part B: Polym Phys* 55(18): p. 1365-1372. <https://doi.org/10.1002/polb.24383>
- [38] Sudduth, R.D (2013) A review of the similarities and differences between five different polymer-solvent interaction coefficients. *Pigment & Resin Technol.* <https://doi.org/10.1108/PRT-07-2012-0042>
- [39] Scott, R.L. and M. Magat (1949) Thermodynamics of high-polymer solutions. III. Swelling of cross-linked rubber. *J Polym Sci* 4(5): p. 555-571. <https://doi.org/10.1002/pol.1949.120040502>
- [40] Blanks, R.F. and J. Prausnitz (1964) Thermodynamics of polymer solubility in polar and nonpolar systems. *Indu & Eng Chem Fundamentals* 3(1): p. 1-8. <https://doi.org/10.1021/i160009a001>
- [41] Bae, Y et al (1993) Representation of vapor–liquid and liquid–liquid equilibria for binary systems containing polymers: applicability of an extended Flory–Huggins equation. *J Appli Polym Sci* 47(7): p. 1193-1206. <https://doi.org/10.1002/app.1993.070470707>
- [42] Favre, E., Clément, R., Nguyen, Q. T., Schaetzel, P., & Néel, J (1993) Sorption of organic solvents into dense silicone membranes. Part 2.—Development of a new approach based on a clustering hypothesis for associated solvents. *J Chem. Soc., Faraday Trans* 89(24), 4347–4353. <https://doi.org/10.1039/FT9938904347>
- [43] Kappert, E.J et al (2019) Swelling of 9 polymers commonly employed for solvent-resistant nanofiltration membranes: A comprehensive dataset. *J Membr Sci*, 569: p. 177-199. <https://doi.org/10.1016/j.memsci.2018.09.059>
- [44] Chilin, C. and A. Metters (2006) Hydrogels in controlled release formulations: Network design and mathematical modelling. *Adv. Drug Deliv. Rev* 58: p. 1379-1408. <https://doi.org/10.1016/j.addr.2006.09.004>
- [45] Wang, C et al (2008) Synthesis and performance of novel hydrogels coatings for implantable glucose sensors. *Biomacromol* 9(2): p. 561-567. <https://doi.org/10.1021/bm701102y>
- [46] Bajpai, A., J. Bajpai, and S. Shukla (2002) Water sorption through a semi-interpenetrating polymer network (IPN) with hydrophilic and hydrophobic chains. *Reacti and Funct Polym* 50(1): p. 9-21. [https://doi.org/10.1016/S1381-5148\(01\)00085-2](https://doi.org/10.1016/S1381-5148(01)00085-2)
- [47] Crini, G (2008) Kinetic and equilibrium studies on the removal of cationic dyes from aqueous solution by adsorption onto a cyclodextrin polymer. *Dyes and Pigments* 77(2): p. 415-426. <https://doi.org/10.1016/j.dyepig.2007.07.001>
- [48] Aminabhavi, T.M. and R.S. Khinnavar (1993) Diffusion and sorption of organic liquids through polymer membranes: 10. Polyurethane, nitrile-butadiene rubber and epichlorohydrin versus aliphatic alcohols (C1-C5). *Polym* 34(5): p. 1006-1018. [https://doi.org/10.1016/0032-3861\(93\)90222-V](https://doi.org/10.1016/0032-3861(93)90222-V)
- [49] Bernardo, G (2013) Diffusivity of alcohols in amorphous polystyrene. *Journal of applied polymer science* 127(3): p. 1803-1811. <https://doi.org/10.1002/app.37918>
- [50] Xu, N. and C. Xiao (2011) Kinetics modeling and mechanism of organic matter absorption in functional fiber based on butyl methacrylate-hydroxyethyl methacrylate copolymer and low density polyethylene. *Polym-Plastics Technol and Eng* 50(14): p. 1496-1505. <https://doi.org/10.1080/03602559.2011.593084>

Table Caption

Table 1 Composition and designation of the homopolymers and the copolymer.

Samples	IBOA (mol. %)	EHA (mol. %)	HDDA (mol. %)	Darocur (mol. %)
poly (IBOA)	99.4	0.0	0.1	0.5
poly (2-EHA)	0	99.4	0.1	0.5
poly (IBOA-co-2-EHA)	56.7	42.7	0.1	0.5

Table 2 Glass transition data of the homopolymer and the copolymer.

Sample	T _g (°C)	Δ C _p (J g ⁻¹ °C ⁻¹)
poly (IBOA)	48.00	0.155
poly (IBOA-co-2-EHA)	4.00	0.157
poly (2-EHA)	-66.00	0.155

Table 3 Solubility parameters of solvent calculated according to Hildebrand and Hansen methods.

Solvents	Hildebrand solubility parameters		Hansen solubility parameters	
	δ _s (J/cm ³) ^{1/2}	δ _d (J/cm ³) ^{1/2}	δ _p (J/cm ³) ^{1/2}	δ _h (J/cm ³) ^{1/2}
Methanol	28.2	15.1	12.3	22.3
Ethanol	25.9	15.8	8.8	19.4
Propan-1-ol	24.2	16.0	6.8	17.4
Butan-1-ol	23.2	16.0	5.7	15.8
Pentan-1-ol	22.5	15.9	5.9	13.9
Hexan-1-ol	21.9	15.9	5.8	12.5
Heptan-1-ol	21.4	16.0	5.3	11.7
Toluene	18.7	18.0	1.4	2.0

Table 4 Density, molar volume and volume fraction of solvent and Flory Huggins parameter interaction.

Solvents	Density (g/cm ³)	V _s (cm ³ /mol)	Φ _s	χ _{scop}	χ
Methanol	0.791	40.7	0,114	1.64	2,29
Ethanol	0.789	58.6	0.138	1.51	2.09
Propan-1-ol	0.804	75.1	0.381	0.90	1.78
Butan-1-ol	0.810	91.5	0,779	0.61	1,62
Pentan-1-ol	0.811	108.6	0.803	0.60	1.52
Hexan-1-ol	0.814	124.6	0,810	0.60	1,40
Heptan-1-ol	0.822	141.7	0,807	0.60	1,30
Toluene	0.865	106.8	0,911	0.53	0,42

Table 5 Diffusion parameter of poly (IBOA-co-2-EHA) in polar and non-polar solvents

Solvents	Methanol	Ethanol	Propan-1- ol	Butan-1- ol	Pentan-1- ol	Hexan-1- ol	Heptan-1- ol	Toluene
n	0.27	0.25	0.38	0.46	0.46	0.42	0.44	0.65
k	0.138	0.108	0.035	0.019	0.012	0.018	0.015	0.025
R ²	0.958	0.981	0.999	0.985	0.971	0.959	0.961	0.991
D (x10 ⁻⁶ cm ² /min)	2.74	2.04	1.15	0.98	0.54	0.52	0.58	11.9

Table 6 Swelling kinetic parameters of poly (IBOA-co-2-EHA) in alcohols.

Alcohols	Experimental SD _e (g solvent /g copolymer)	k' (x 10 ⁻⁴ g copolymer / (g solvent min)	Calculated SD _e (g solvent /g copolymer)	R ²
Methanol	0.111	217	0.113	0.995
Ethanol	0.150	75.07	0.151	0.942
Propan-1-ol	0.575	35.69	0.595	0.996
Butan-1-ol	3.601	3.33	3.820	0.995
Pentan-1-ol	3.800	1.84	4.170	0.977
Hexan-1-ol	4.100	1.53	4.509	0.980
Heptan-1-ol	4.310	1.48	4.77	0.983
Toluene	10.68	8.39	10.98	0.999

Figure Captions

Fig. 1 Chemical structures of reactants used in the elaboration of polymers: a) 2-EHA, b) IBOA and c) HDDA.

Fig. 2 Computer-generated and energy-minimized representation of 40 units: a) poly (2-EHA) and b) poly (IBOA) respectively. The ball and stick models were generated with Chem3D.16.0 software. (Oxygen atoms in red, carbon atoms in gray, hydrogen atoms in white)

Fig. 3 Superposition of FTIR spectra before ($t=0$ min) and after irradiation ($t=30$ min) for: a) poly (2-EHA), b) poly (IBOA-co-2-EHA), and c) poly (IBOA). The inserts show the reduction of C=C double bond before and after UV exposure.

Fig. 4 DSC thermograms of the homopolymers: poly (IBOA), poly (2-EHA) and poly (IBOA-co-2-EHA).

Fig. 5 Photos of poly (IBOA-co-2-EHA) swollen in toluene at different times.

Fig. 6 Swelling behavior of poly (IBOA-co-2-EHA) as function of immersion time for different solvents à $T=25^{\circ}\text{C}$.

Fig. 7 Swelling behavior of poly (2-EHA), poly (IBOA-co-2-EHA) and poly (IBOA) as function of immersion time à $T=25^{\circ}\text{C}$ in (a) Toluene and (b) Heptan-1-ol.

Fig. 8 Swelling degree (left) and poly (IBOA-co-2-EHA) / solvent interaction parameter (right) versus solubility parameters of pure solvents. (1: Methanol, 2: Ethanol, 3: Propan-1-ol, 4: Butan-1-ol, 5: Pentan-1-ol, 6: Hexan-1-ol, 7: Heptan-1-ol and 8: Toluene).

Fig. 9 Photos of copolymer swollen at $T=25^{\circ}\text{C}$ in a) Methanol and b) Heptan-1-ol.

Fig. 10 Second-order kinetics plots for poly (IBOA-co-2-EHA) swollen in different solvents, at 25°C .

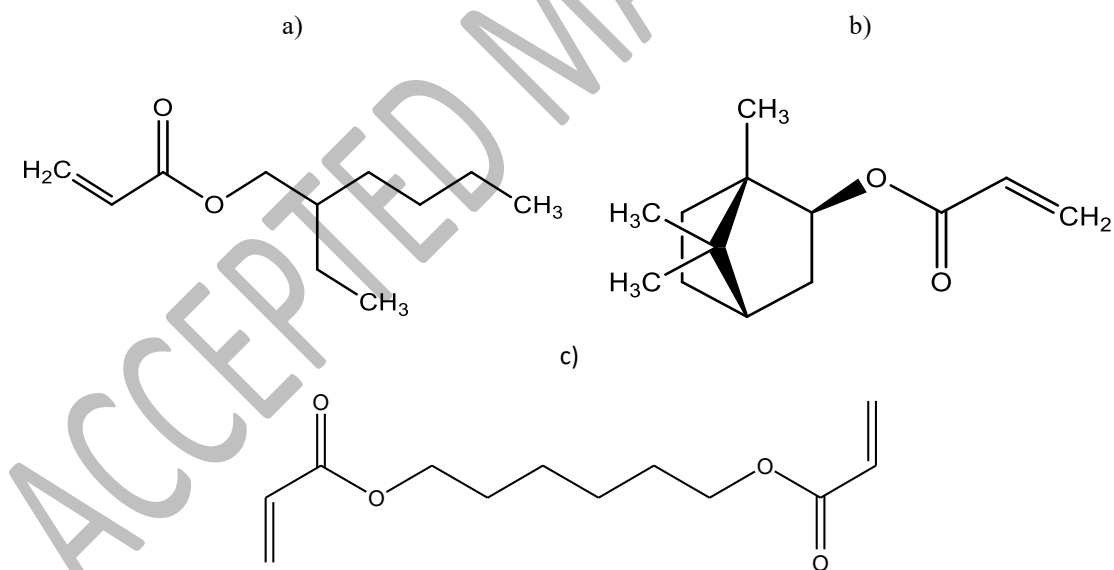


Fig.1

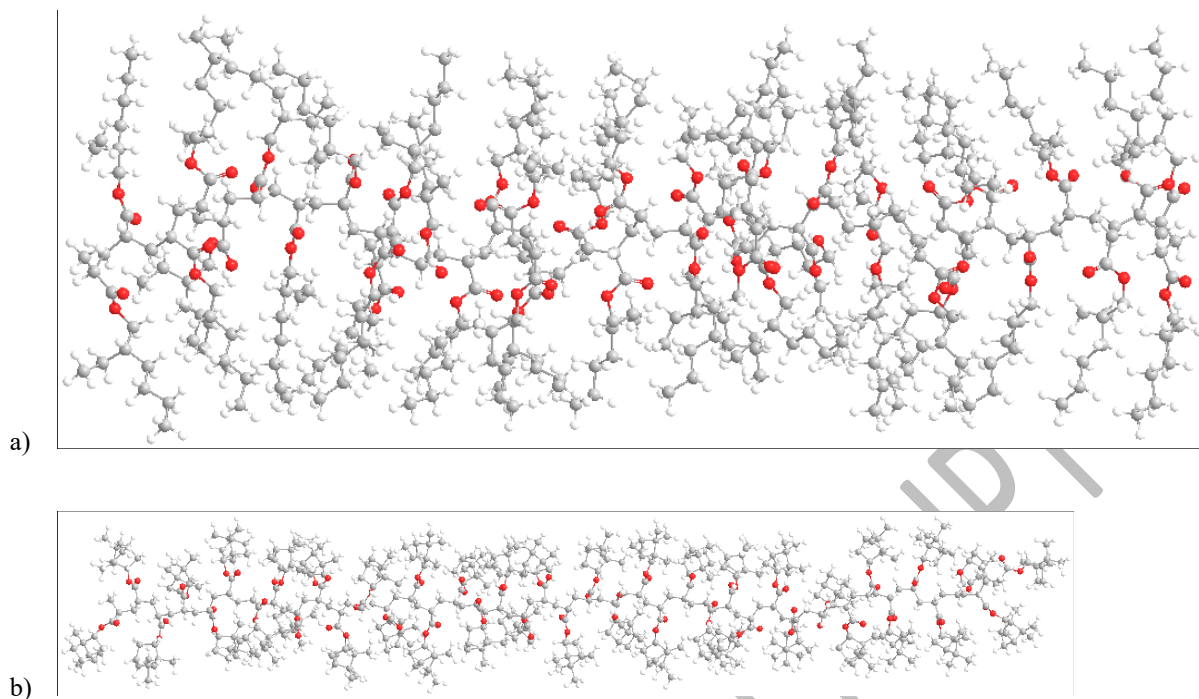
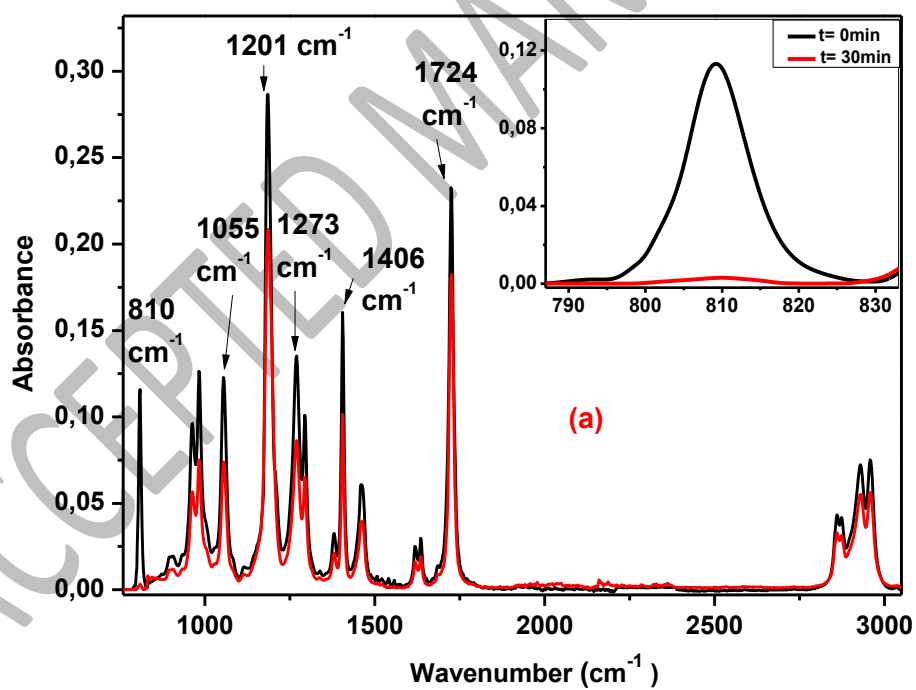


Fig. 2



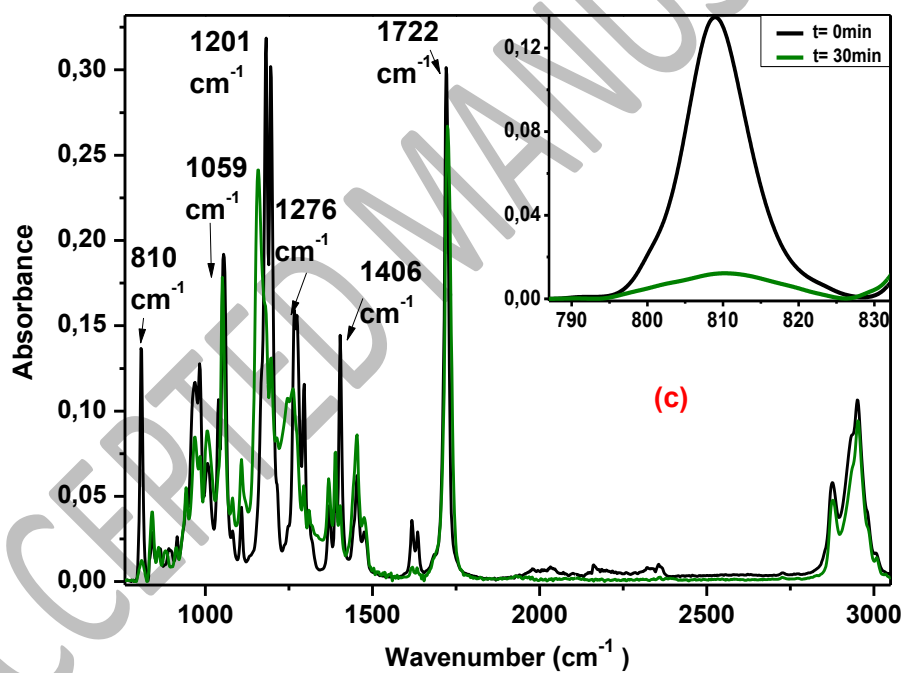
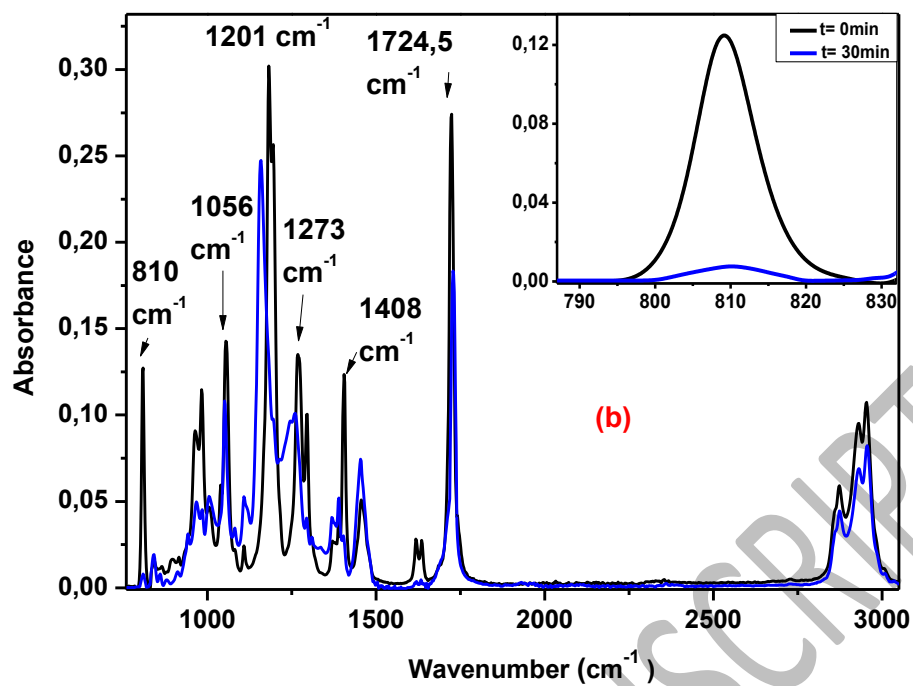


Fig. 3

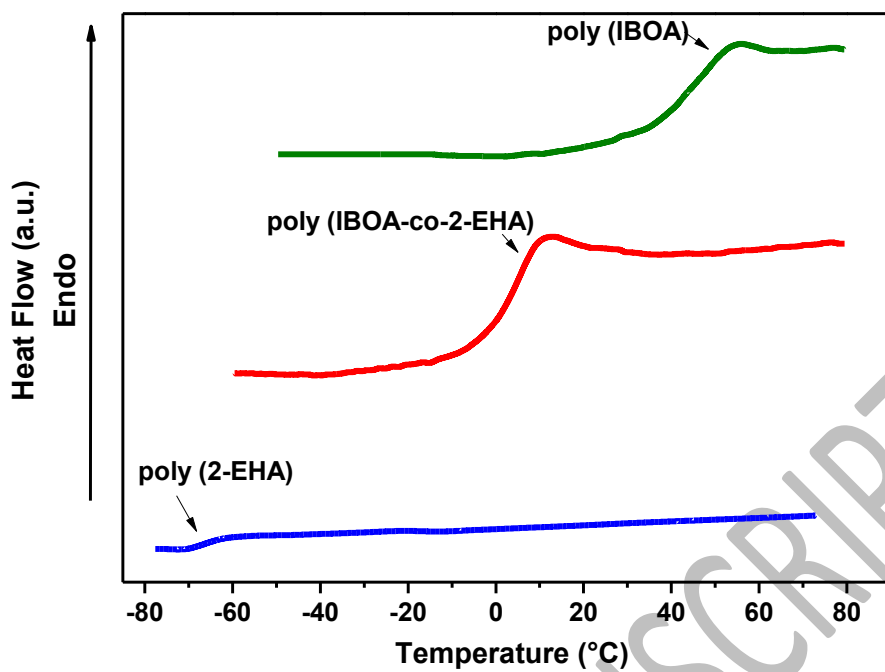
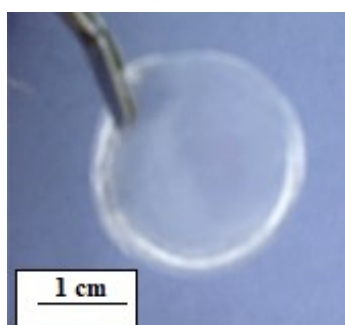
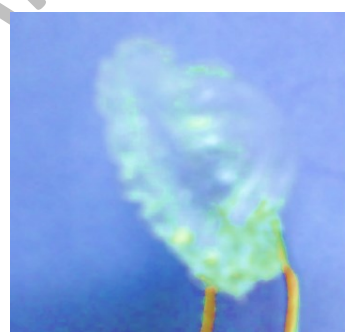


Fig. 4



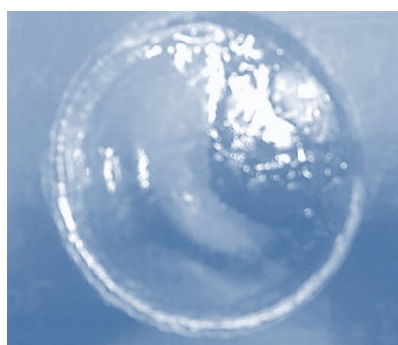
t=0 min



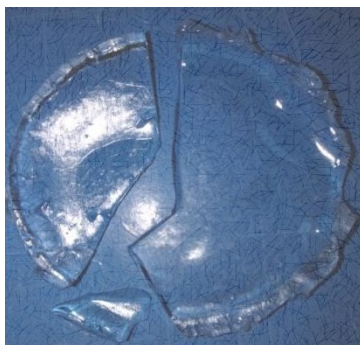
t=10 min



t = 15 min



t = 30 min



t = 24h

Fig. 5

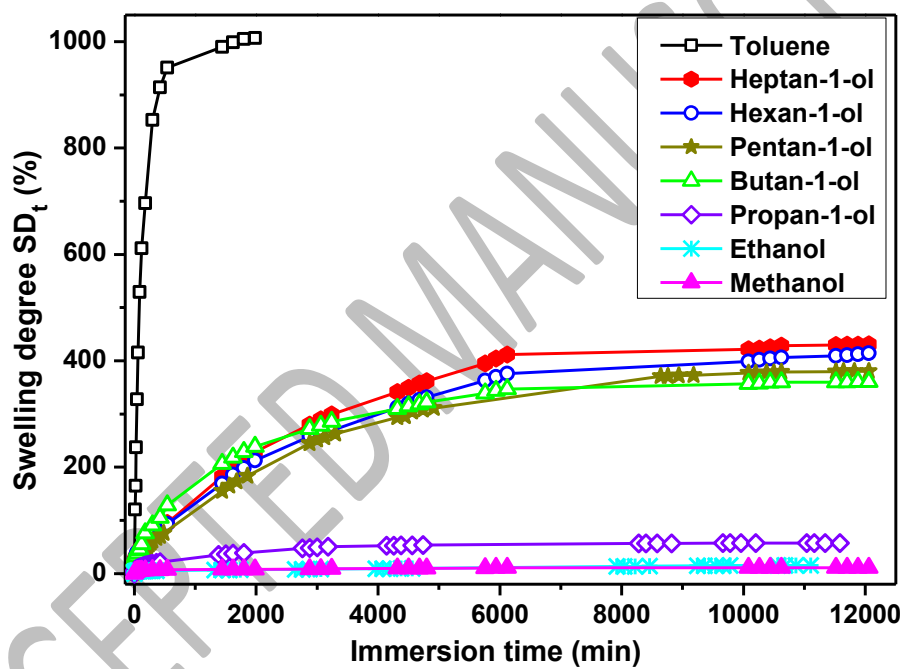


Fig. 6

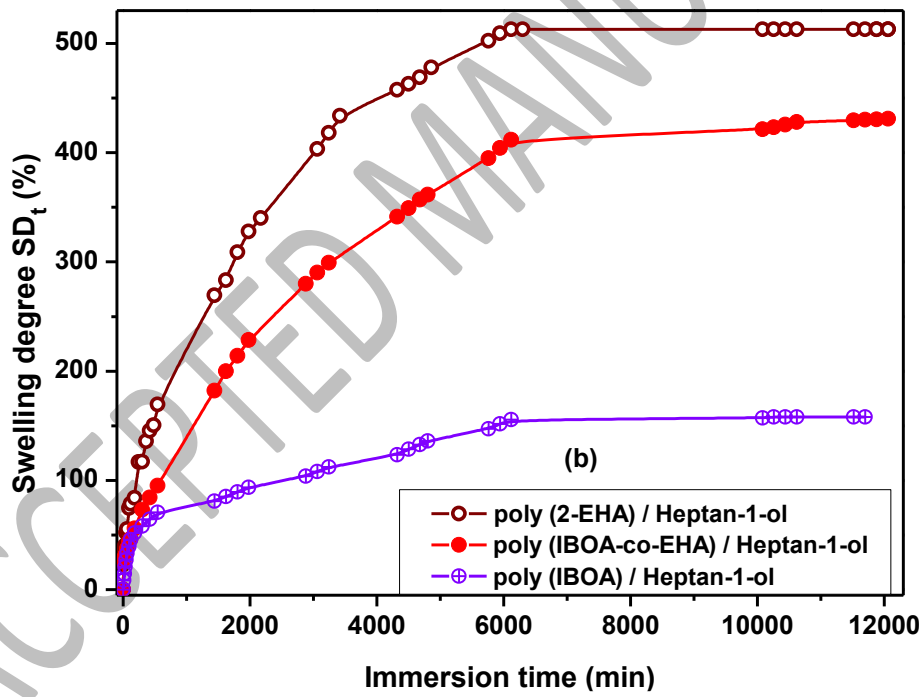
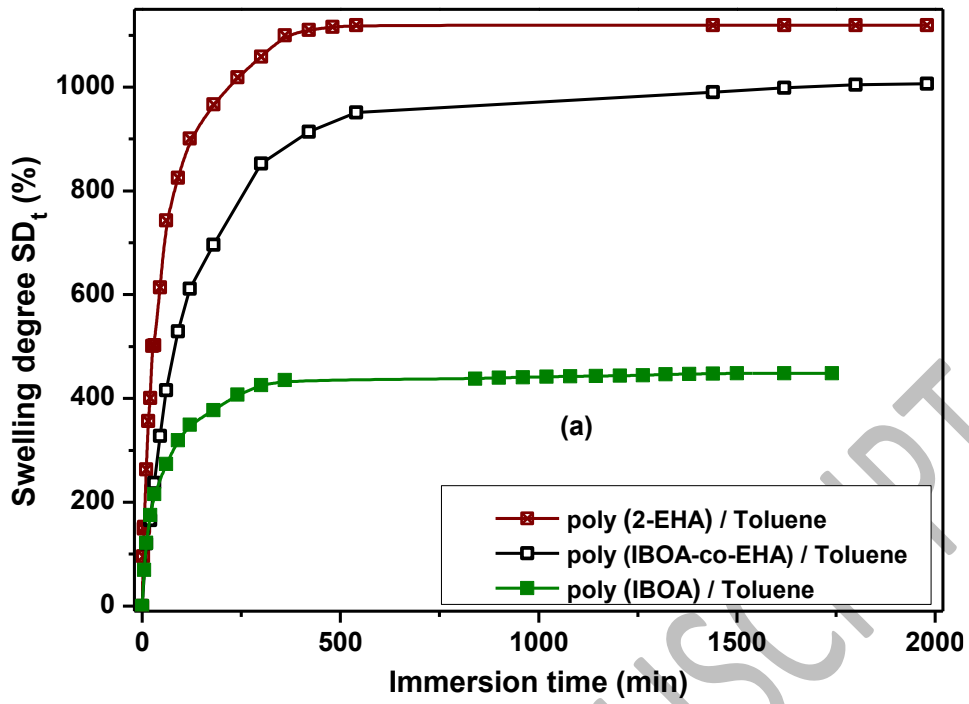


Fig. 7

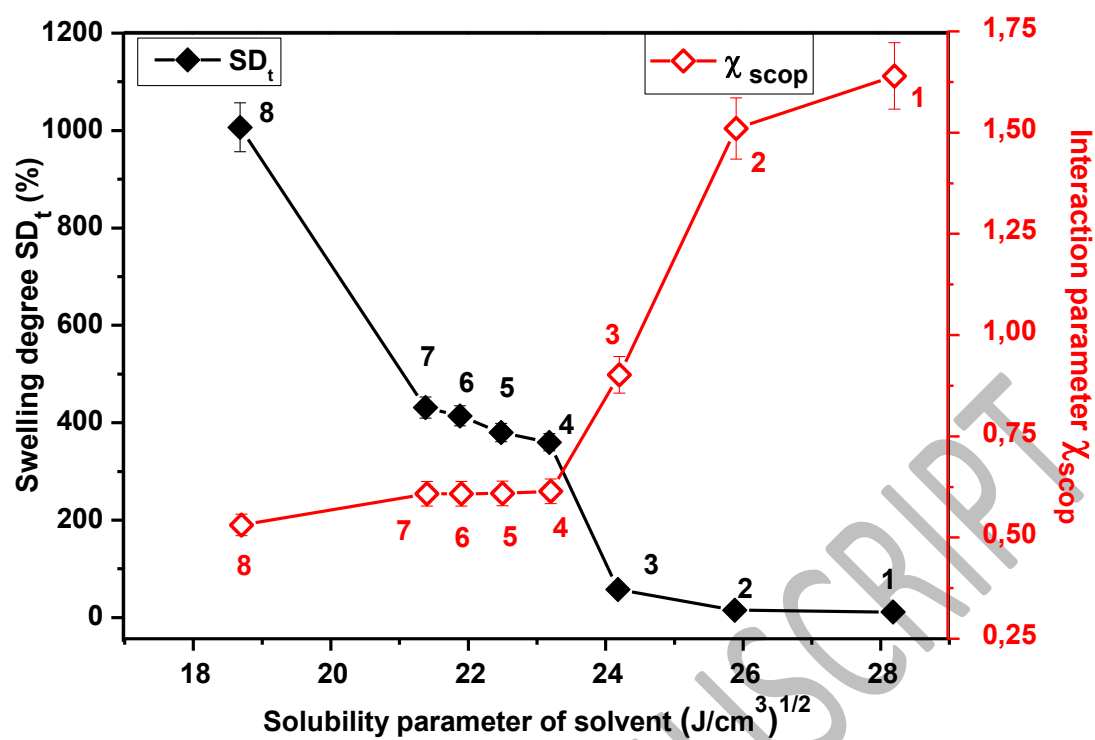


Fig. 8

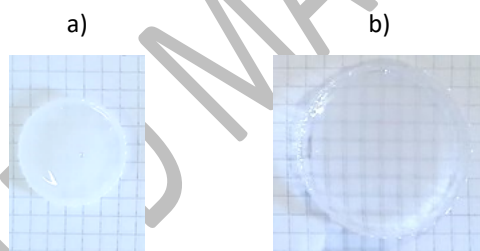


Fig. 9

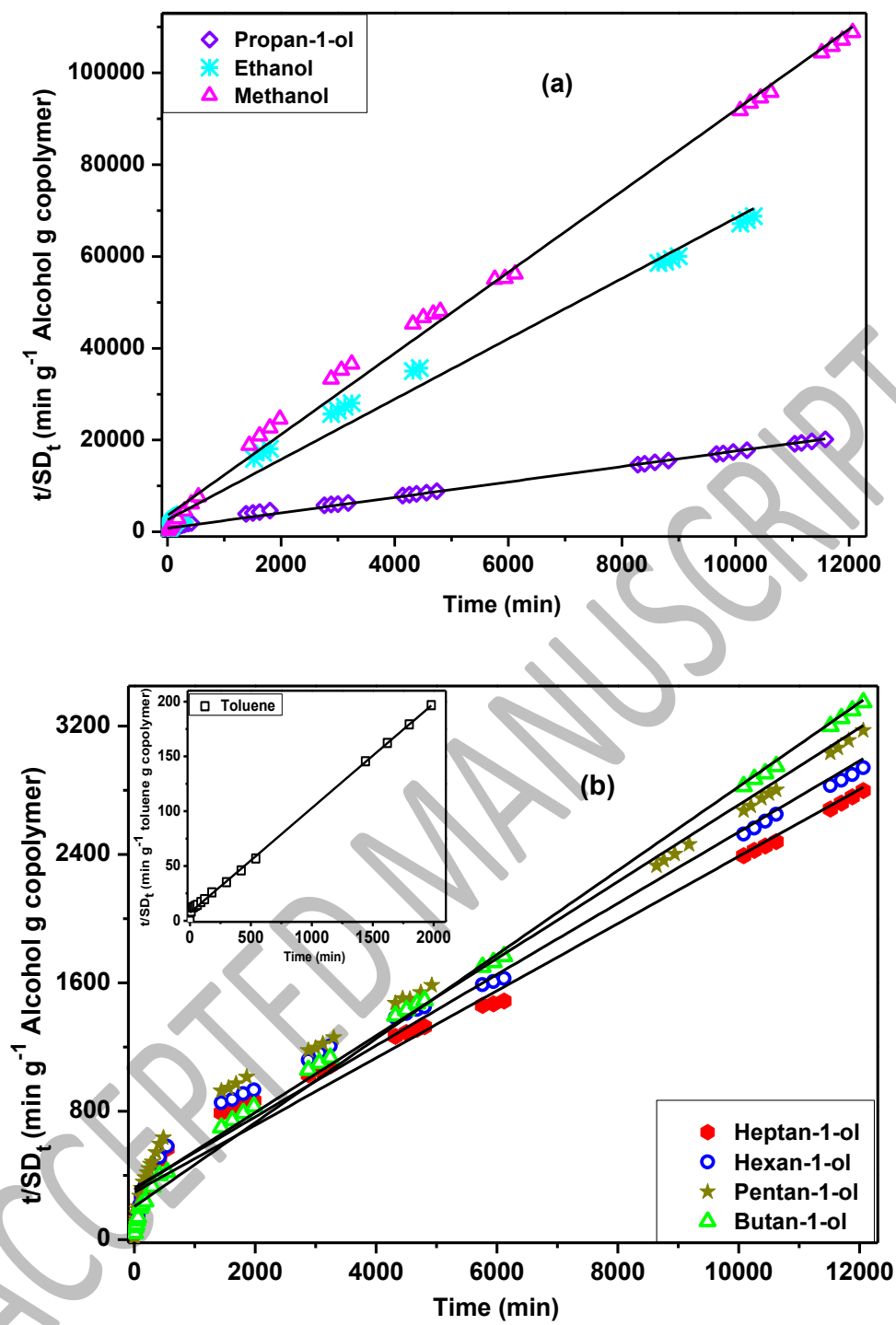


Fig. 10